FINITE ELEMENT ANALYSIS OF HUMAN AND ARTIFICIAL ARTICULAR CARTILAGE

Dr. Sadiq Jafer Abbass
College of Engineering
Nahrain University

Eng. Farah Mohammed Reda Abdulateef
College of Engineering
Nahrain University

Joint diseases, such as osteoarthritis, induce pain and loss of mobility to millions of people around the world. Current clinical methods for the diagnosis of osteoarthritis include X-ray, magnetic resonance imaging, and arthroscopy. These methods may be insensitive to the earliest signs of osteoarthritis. This study investigates a new procedure that was developed and validated numerically for use in the evaluation of cartilage quality. This finite element model of the human articular cartilage could be helpful in providing insight into mechanisms of injury, effects of treatment, and the role of mechanical factors in degenerative conditions, this three-dimensional finite element model is a useful tool for understanding of the stress distributions within articular cartilage in response to external loads and investigating both the prevention of injury and the pathological degeneration of the joints.

In this study, 21 models were analysed by using ANSYS workbench v12.1: four normal articular cartilage models (distal femur, patella, medial and lateral tibia). A redesign to the distal femur model was done to get osteoarthritis articular cartilage (simple and deep) seven models by making partial cut without affecting the subchondral bone, and full cut with part of the subchondral bone in different diameters. Finally a treatment done by replacing the defective parts with artificial articular cartilages with different types of treatment. The finite element analysis studied depending on a Von Mises criteria and total deformation in different activities. The results shows that Autologous Chondrocyte Implementation is the best treatment way and it is close by 87.50% to normal cartilage. This procedure can be used as a diagnostic procedure for osteoarthritic patients and to choose the best treatment options.

الخلاصـــــــة

أمراض المفاصل، كـ (إلتهاب المفاصل الضموري)، تسبب الالم وعدم القدرة على الحركة لملايين الناس في العالم. طرق التشخيص الحالية للمرضى تستخدم الاشعة السينية، و جهاز الرنين المغناطيسي، و الناظور المفصلي، هذه الطرق لا تكون حساسة لإكتشاف العلامات الاولى لحدوث هذا المرض. لذلك هذه الدراسة بحثت طريقة جديدة طُورت حسابياً لتستخدم في تقييم كفاءة الغضروف عن طريق تصميم نموذج للغضروف المفصلي في الانسان بإستخدام العناصر المحددة لإلقاء الضوء على ميكانيكية الجرح و تأثيرات المعالجة و دور العوامل الميكانيكية في حدوث الأضرار و يعتبر نموذج العناصر المحددة ثلاثي الابعاد للغضروف المفصلي هذا طريقة مفيدة في فهم توزيع الاجهاد ضمن الغضروف المفصلي ضد الاجهادات الخارجية و بحث كل من منع حدوث الاضرار والامراض التي تحدث في المفاصل. في هذه الدراسة تم تحليل واحد وعشرون نموذجاً بإستخدام برنامج (ANSYS workbench v12.1) يتضمن أربع نماذج للغضروف المفصلي الطبيعي (غضروف عظم الفخذ السفلي، و غضروف الرضفة، و غضروفي عظم القصبة الداخلي والخارجي)، وبعدها تم إزالة جزء من الغضروف المفصلي لعظم الفخذ ليصبح كأنه مصاب بمرض (إلتهاب المفاصل الضموري) البسيط والعميق وذلك عن طريق عمل قطع جزئي بدون التأثير على العظم الذي تحت الغضروف، ومن ثم عمل قطع كامل لجزء من الغضروف مع جزء من العظم الذي تحته، وبأبعاد مختلفة بكلتا الحالتين، ثم معالجة الجزء المقطوع بإستبداله بغضروف مفصلي صناعي بإستخدام عدة طرق للعلاج ثم دراسة التحليل بإستخدام العناصر المحددة بالاعتماد على معايير (Von Misses) و التشوه الكلي في نشاطات مختلفة.

Key Words:
Finite element analysis, Articular Cartilagr, Artificial AC, Osteoarthritis, Arthritis, ANSYS.

Introduction

Articular cartilage is a complex tissue, which covers the ends of long bones in synovial joints. It protects the subjacent bone from high friction, increases contact area, and consequently improves the local joint congruence [C. Bratianu 2004][J. Yao 2003]. Articular cartilage is a biphasic material that consists of a solid and a fluid phase. As a result of this biphasic structure articular cartilage is viscoelastic [G. Li 1998]. Cartilage plays an extremely important role within the bod
y's joints [W. Bogatay 2009]. In combination with the synovial fluid, articular cartilage enables furthermore a nearly frictionless movement of the joint over the whole lifespan of a person. As articular cartilage has only a limited capacity for self-repair, this process, once started, can hardly be reversed [S. Knecht 2006]. It has been well established that articular cartilage is compositionally and mechanically inhomogeneous through its depth [R. Krishnan 2003]. This unique structure generates a complex mechanical response under physiological or extreme loads related to sports activities. Therefore, an accurate understanding of the joint biomechanics considerably improves the prevention and treatment of the joint disorders and injuries [C. Bratianu 2004]. Calculating cartilage stress is technically challenging, as many factors can influence stress, including the joint contact force, material properties of the tissue, the geometry of the articulating surfaces, and the cartilage thickness [T. Besier 2005].

Articular Cartilage Structure

In normal human joints, the thickness of the articular cartilage layer varies from 0.5 to 1.5 mm in upper extremity joints and from 1 to 6 mm in lower extremity joints [8, 9]. Structure and components of synovial joint are shown in **Figure** (1). Furthermore, articular cartilage distributes the loads over a larger contact area, thereby minimizing the contact stress, and absorbing part of the energy transferred through the joints during normal activities [D. Schneck 2003].

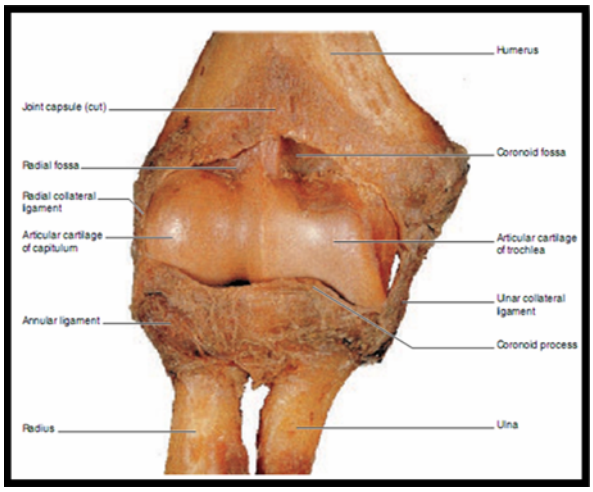

Figure (1) Structure and components of synovial joint (elbow joint) [V. Graaff 2001].

Articular cartilage plays a vital role in the function of the musculoskeletal system by allowing almost frictionless motion to occur between the articular surfaces of a diarthrodial joint for smooth joint movement [A. Iftekhar 2004], The coefficient of friction between articulating surfaces is remarkably low during dynamic loading (in human joints 0.001 - 0.08).

The low coefficient of friction results from the biphasic nature of cartilage and the lubrication induced by the synovial fluid [T. Besier 2005][W. Wilson 2005].

Articular or hyaline cartilage forms the bearing surfaces of the movable joints of the body. The importance of articular cartilage as a bearing surface has led to extensive mechanical and tribologic studies of this tissue [J. Black 1998]. **Figure** (2) shows the structure of the synovial joint.

Due to the avascular nature of articular cartilage, the provision of metabolites to the cells is assumed to occur via diffusion from the synovial fluid or, to a lesser extent, the underlying bone. However, the lack of blood supply severely diminishes the ability of cartilage to heal once it has been damaged [S. Knecht 2006][A. Iftekhar 2004].

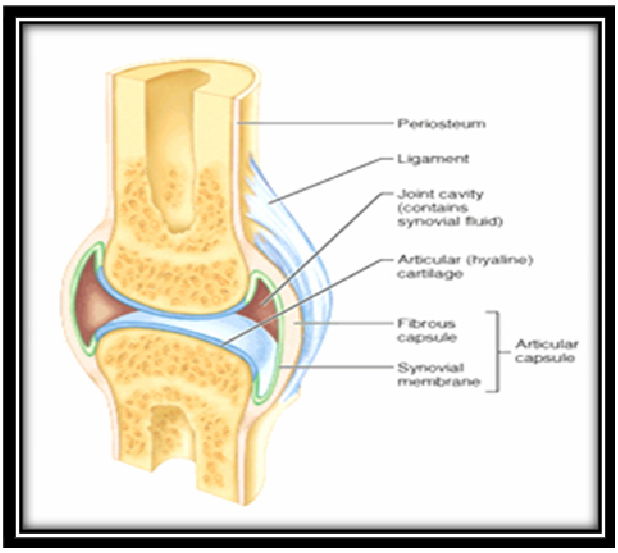

Figure (2) Structure of the synovial joint [T. Gill 2006].

The cartilage does not possess a uniform thickness. It is influenced by different factors, e.g., size of bone, pressure, stress, and age [M. Mlejnek 2006]. The interactions between collagen, proteoglycans, and fluid play an important role in the mechanical response of cartilage [T. Besier 2005].

Organization of the articular cartilage

The structural arrangement of the biochemical components in articular cartilage is highly anisotropic and inhomogeneous. Based on its composition and orientation of the components with depth of the tissue, articular cartilage is divided into a superficial zone, a middle zone, a deep zone, and a calcified cartilage zone [A. Bhosale 2008]. The four zones of the articular cartilage are shown in **Figure** (3).

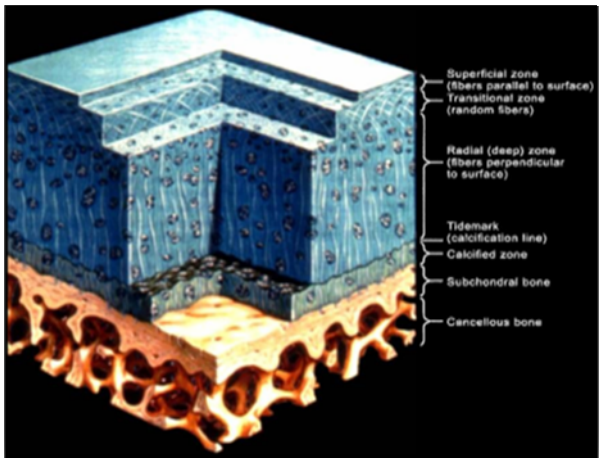

Figure (3) The four zones of the articular cartilage [W. Wilson 2005].

Articular cartilage damage and repair

Degenerative arthritis is an enormous problem, which affects millions of people around the world [W. Holmes 2004]. The overall prevalence for moderate to severe osteoarthritis is approximately 20%. By the age 55-65, up to 85% of all people will have some degree of osteoarthritis in one or more joints [F. DT 1997].Example of osteoarthritic articular cartilage is shown in **Figure** (4).

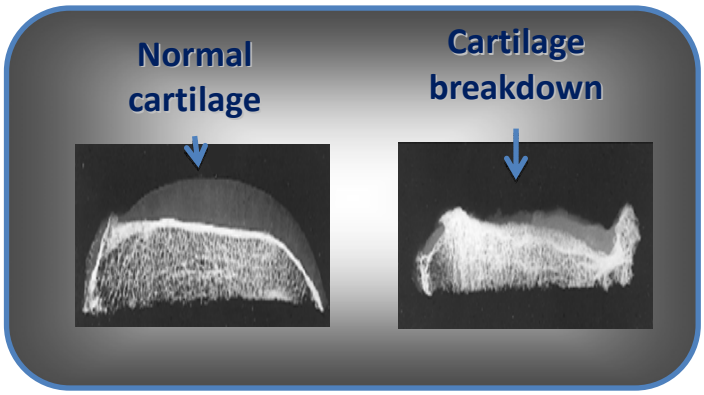

Figure (4) Normal and osteoarthritic articular cartilage (patella) [Janssen 2004].

Articular cartilage damages

Surgeons classify defects in the knee cartilage using a grading scale from I to IV. In grade I tear, the cartilage has a soft spot. Grade II lesions show minor tears in the surface of the cartilage. Grade III lesions have deep crevices. In grade IV lesions, the tear goes all the way to the underlying bone, as shown in **Figure** (5).

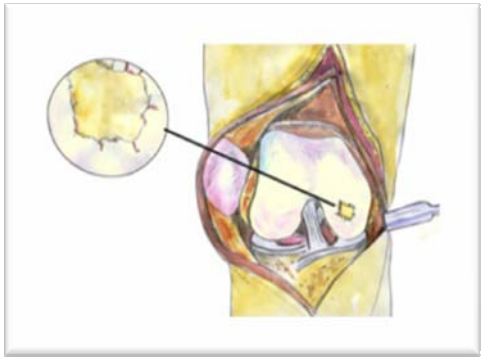

Figure (5) Knee cartilage lesions [T. Besier 2005].

A grade IV lesion goes completely through all layers of the cartilage. It is diagnosed as a full-thickness lesion. Sometimes part of the torn cartilage will break off inside the joint. Since it

is no longer attached to the bone, it can begin to move around within the joint, causing even more damage to the surface of the cartilage. Some doctors refer to this unattached piece as a loose body [Orthopod 2003].

Cartilage lacks a supply of blood or lymph vessels, which normally nourish other parts of the body. Without a direct supply of nourishment, cartilage is not able to heal itself if it gets injured [Orthopod 2003].

Treatment of articular cartilage injuries

The treatment of articular cartilage injuries is made in two ways, operative and non-operative treatments.

Nonsurgical Treatment

Nonsurgical management includes oral medications, physical modalities (physical therapy, weight loss), bracing (knee sleeve and unloaded brace), and injections (corticosteroids and hyaluronic acid derivatives). Traditionally, treatment of articular cartilage lesions has included a combination of nonsteroidal anti-inflammatory drugs, activity modification, and oral chondroprotective agents such as glucosamine or chondroitin sulfate. Such management is often ineffective in highly active and symptomatic patients and may only prove beneficial in low-demand patients [T. Pylawka 2004].

Surgical Treatment

The spectrum of different cartilage repair approaches has considerably been increased in the recent years [Gelse K. 2010]. The treatment options to restore the articular cartilage surface involve consideration of many factors: defect size, depth, location, response to previous treatment, patient age and expectations [T. Pylawka 2004].

1. Arthroscopic debridement and lavage

Arthroscopic lavage entails inserting arthroscopic instruments into the knee and irrigating the joint with sterile fluid, as shown in **Figure** (6).

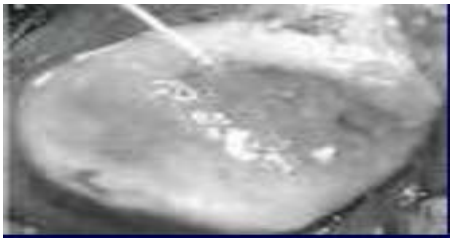

Figure (6) Arthroscopic debridement and lavage [R. Baxter 2008].

2. Repair stimulation techniques

Repair stimulation techniques try to take advantage of the normal tissue repair processes to create a new joint surface. [W. Holmes 2004].

a. Drilling

The subchondral plate is penetrated using a drill, the subchondral bone is drilled with a 0.185-cm drill to stimulate a fibrocartilagenous repair of a full-thickness chondral defect [T. Gill 2006].

b. Microfracture

This surgery, which aims to stimulate blood flow and promote regeneration, is a popular procedure for young patients but it is not performed on patients in their forties or fifties. A surgical procedure that can help such a patient is osteochondral autograft replacement [W. Bogatay 2009].

c. Abrasion arthroplasty

When osteoarthritis affects a joint, the articular cartilage can wear away, leaving bone rubbing on bone. This causes the bone to become hard and polished. During arthroscopy the surgeon can use a special instrument known as a burr to perform an abrasion arthroplasty, as shown in **Figure** (7).

In this procedure, the surgeon carefully scrapes off the hard, polished bone tissue from the surface of the joint. The scraping action causes a healing response in the bone. In time, new blood vessels enter the area and fill it with fibrocartilage [Orthopod 2003].

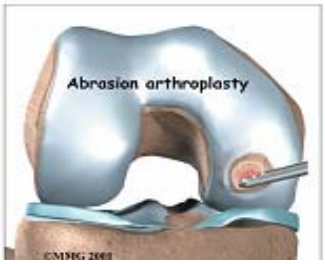

Figure (7) Abrasion arthroplasty [Orthopod 2003].

3. Cell and tissue transplantation

These techniques show promise in recreating a new articular surface with similar properties to native articular cartilage.

a. Osteochondral autografting

An autograft is a procedure for grafting tissue autograft from the patient's own body [Orthopod 2003].

b. Osteochondral allografting

An allograft is a lot like the osteochondral autograft, but instead of taking tissue from the patient's donor site, surgeons rely on tissue from another person, much like using donor hearts, kidneys, and other organs [Orthopod 2003].

c. Autologous chondrocyte implantation

Autologous chondrocyte implantation is a two-stage procedure involving a biopsy of normal articular cartilage, usually obtained through an arthroscopic procedure, in which the cartilage is harvested from a minor load-bearing area (upper medial femoral condyle or intercondylar notch). These chondrocytes are then cultured in vitro and implanted into the chondral defect beneath a periosteal patch during a second-stage procedure that requires an arthrotomy [T. Pylawka 2004]. Surgeons may recommend this procedure for active, younger patients (20 to 50 years old) when the bone under the lesion hasn't been badly damaged [Orthopod 2003].

4. Soft tissue replacement (polymers for cartilage replacement)

Replacement or augmentation of orthopedic soft tissues can be used to treat injury or disease-based degradation to the original tissue. Osteoarthritis characterized by degradation of the articular cartilage that progresses to the bony surfaces themselves is one of the most common pathologies experienced by the aging population. The density of polyethylene has been increased and joint bearings are now typically constructed from ultra-high-molecular-weight polyethylene (UHMWPE). The material has proven to provide good articulation, with the main concern being long-term wear. The problem with wear is not only the mechanical impingement that can occur as a result of a change in the articulating surface geometry but, more importantly, the effect of wear debris on the surrounding tissue [M. Grimm 2004].

Articular Cartilage Biomechanics

The histologic structure of articular cartilage is influenced by the local mechanical loading of chondrocyte in the different zones [U. Meyer 2006]. Because the fluid primarily is exuded from the surface layer, the distribution of strains through the cartilage thickness is highly nonuniform (**Figure** 8). Tissue results in compressive strains of over 50% in the superficial cartilage zone, but these strains reduce to near zero in the middle and deep regions of cartilage [D. Carter 2004].

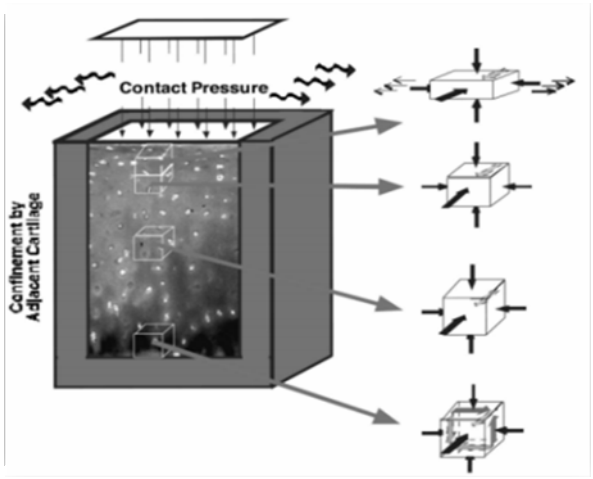

Figure (8) Schematic representation of the mechanical environment of articular cartilage under intermittent joint loading and motion [D. Carter 2004].

Chondrocytes are directly attached to the extracellular matrix and can be considered part of the fluid continuum of cartilage tissue. The zonal structure of articular cartilage is essential to its ability to support physiologic joint forces. Patterns of stress, strain, and fluid flow created in the joint result in spatial and temporal alteration in chondrocyte function. The external forces are transmitted through the joint and the adjacent tissues resulting in the generation of pressure over contact area of the two opposing cartilage surfaces [U. Meyer 2006], Nonlinear stress–strain curve for pure collagen employed for articular cartilage fibrils showen in (**Figure** 9).

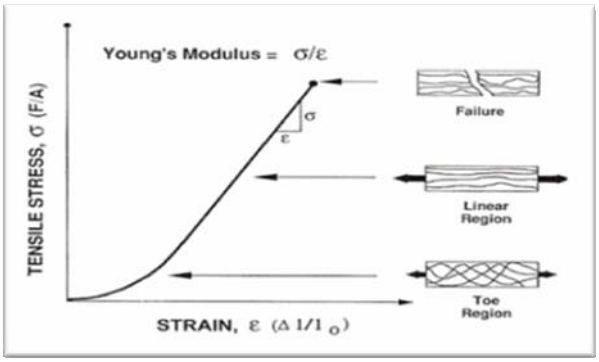

Figure (9) Nonlinear stress–strain curve for pure collagen employed for articular cartilage fibrils. The slope of the curve monotonically increases at smaller strains and becomes constant at larger strains [B. Nigg 1999].

Loads tend to deform the cartilage tissue but these compressive loads and subsequent tissue deformations are resisted by the stress in the solid phase, and the generation of the fluid pressure,and the restriction of tissue deformation by impermeable subchondral bone and the surrounding adjacent cartilage surfaces (**Figures** 10-14) [U. Meyer 2006].

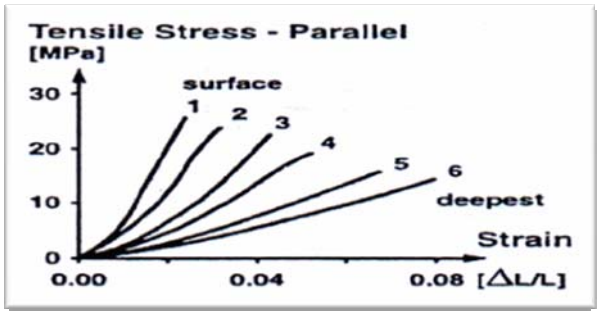

Figure(10) Variation in tension stress behaviour with depth in articular cartilage parallel to the predominant fiber direction [B. Nigg 1999].

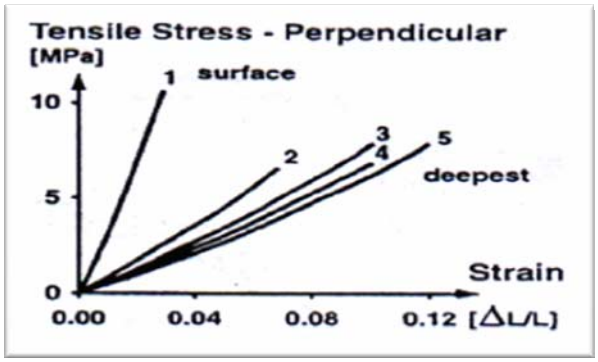

Figure (11) Variation in tension stress behaviour with depth in articular cartilage perpendicular to the predominant fiber direction [B. Nigg 1999].

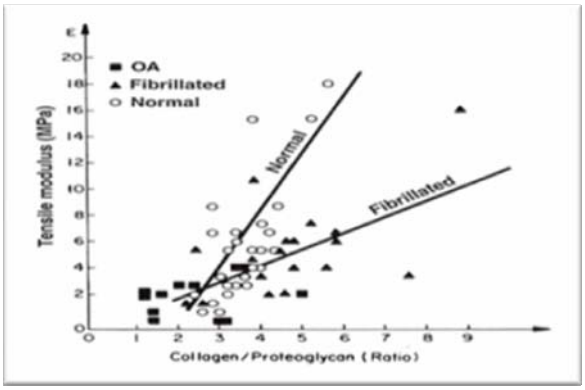

Figure (13) The variation of the human knee joint cartilage tensile stiffness for normal, fibrillated, and osteoarthritic articular cartilage [B. Nigg 1999].

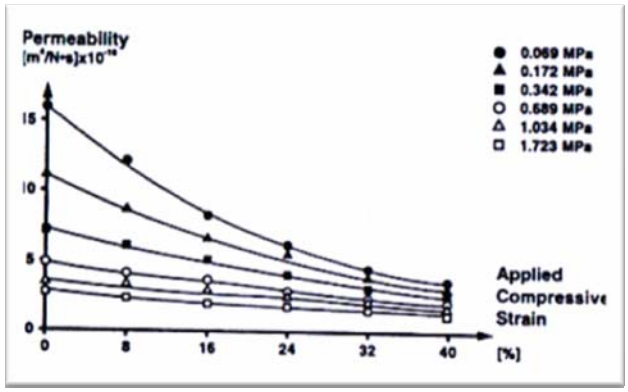

Figure(14) Expermental curves for articular cartilage permeability show a strong dependance on compressive strain and applied pressure [B. Nigg 1999].

Biomaterial Properties of Articular Cartilage

Cartilage behaves as a fiber-reinforced, porous, and permeable composite material. The greatest indicator of the mechanical properties of cartilage is the water content. The modulus of the material decreases with increased water content in a linear relationship. Articular cartilage exhibits both a viscoelastic and a biphasic response under tension, compression, and shear. In this model, the solid phase of articular cartilage is modeled as a hyperelastic anisotropic material. Cartilage exhibits its viscoelastic behavior because of the fluid flow of the liquid phase through the solid phase of the tissue [S. Fening 2005]. Material testing to determine the coefficients in a proposed constitutive law of cartilage is usually through confined compression, unconfined compression and indentation tests (**Figure**15) [S. Knecht 2006].

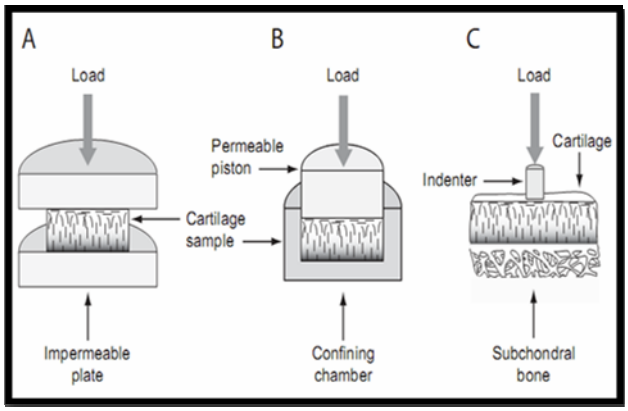

Figure (15) Sketch of common experiments applied to articular cartilage: unconfined compression (A), confined compression (B), and indentation (C) [S. Knecht 2006].

Articular Cartilage Finite Element Analysis

To study the finite element analysis for human articular cartilage, the
articular cartilages of the knee was chosen (the intermediate joint of the lower limb) because it is the largest and most complex joint in the body and containing four articular cartilages (distil femur, medial and lateral proximal tibia, and patella) [A. Iftekhar 2004]. Because the articular cartilages have no exact dimensions and their thickness is changing from place to other and in the cartilage itself so the only way to draw the articular cartilage is by using MRI images. MRI images for articular cartilage were taken from healthy volunteer person with (70 kg) weight and (169 cm) height, and by using a (Syngo FastView software) the images that have the best resolution were taken to be used, then imported as DICOM format in the (SimpleWare software), by using this software the three-dimensional model of the articular cartilages was drawn, then the result was imported in the (AutoCAD 2008) to rearrange the model and finally the last model was imported in the (ANSYS Workbench v 12.1) in order to build three dimensional finite element model which the load will be applied to.

In this work, there are (21) models including: (4) models for normal articular cartilage, (7) models for osteoarthritic articular cartilage, and (10) models for artificial articular cartilage. Each model was studied in two activities (walking and squatting).

Materials properties

Depending on the physical properties it can be seen that the articular cartilage is anisotropic material, the material properties are changing with thickness so the Young's modulus and Poisson's ratio are considered depth-dependent change when moving from lowermost layer at the subchondral bone to the articular surface depending on the organization of the articular cartilage. The superficial articular cartilage layer material characteristics are transversely isotropic poroelastic material (representing 20% of the total articular cartilage thickness), The middle and deep zone articular cartilage layers are isotropic poroelastic material (representing 75% of the total articular cartilage thickness), the calcified cartilage (representing 5% of the total articular cartilage thickness) and bone are elastic material, and finally the fibrocartilage is transversely isotropic elastic material [J. Yao 2003][A. Iftekhar 2004][A. Bhosale 2008]. The material properties for articular cartilage layers, bone, and fibrocartilage are shown in **Table (1),** and the material properties for UHMWPE that was used for total articular cartilage replacement are shown in **Table (2)**.

Table (1) Material properties [J. Yao 2003][A. Iftekhar 2004][A. Bhosale 2008]

	Elastic or Young's Modulus (MPa)	Poisson's Ratio	Permeability (m^4/Ns)	Shear modulus (MPa)
Cartilage (Superficial layer)	$E_x=E_y=5.8$, $E_z=0.46$	$\nu_{xy}=0.0002$ $\nu_{yz}=0$	$k=5.1*10^{-15}$	$G_{xz}=0.20$
Cartilage (Middle and deep zone layers)	E=0.69	$\nu=0.018$	$k=3*10^{-15}$	-
Calcified Cartilage	E=10	$\nu=0.499$	-	-
Bone	E = 220	$\nu=0.3$	-	-
Fibrocartilage	$E_x=100$, $E_y=E_z=0.075$	$\nu_{xy}=0.001$ $5\nu_{yz}=0.5$	-	-
Normal synovial fluid	Elasticity (Pa)	77		
	Viscosity	45		
Osteoarthritic synovial fluid	Elasticity (Pa)	9		
	Viscosity	5		

Table (2) UHMWPE Material Properties [S. Kurtz 2004].

UHMWPE Material Properties	
Young's Modulus (GPa)	0.8
Poisson's Ratio	0.46
Tensile Yield Strength (MPa)	21
Tensile Ultimate Strength (MPa)	21

Creating Mesh

The mesh for the model was done with three dimensional 10-Node Tetrahedral Structural Solid element type (SOLID 187), the shape of the element is shown in **Figure**(16).

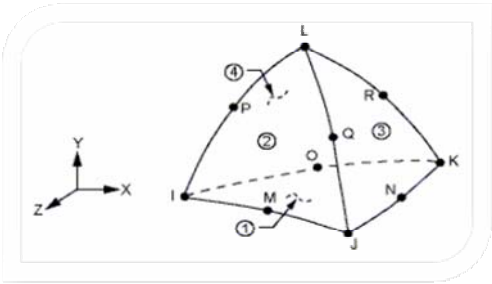

Figure(16) SOLID 187 element shape [S. Leffler 2009].

The reason for choosing (SOLID 187) that it has a quadratic displacement behavior and is well suited to modeling irregular meshes (such as those produced from various CAD systems).
The element is defined by 10 nodes having three degrees of freedom at each node: translations in the nodal x, y, and z directions.
The element has plasticity, hyperelasticity, creep, stress stiffening, large deflection, and large strain capabilities. It also has mixed formulation capability for simulating deformations of nearly incompressible elastoplastic materials, and fully incompressible hyperelastic materials. In addition to the nodes, the element input data includes the orthotropic or anisotropic material properties. Orthotropic and anisotropic material directions correspond to the element coordinate directions [S. Leffler 2009]. The finite element model mesh for distal femur articular cartilage, patella articular cartilage, medial tibia articular cartilage, and lateral tibia articular cartilage are shown in **Figures** (18-21).

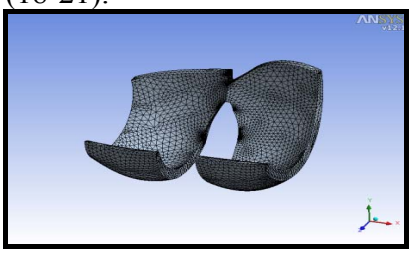

Figure (18) Distal femur articular cartilage mesh.

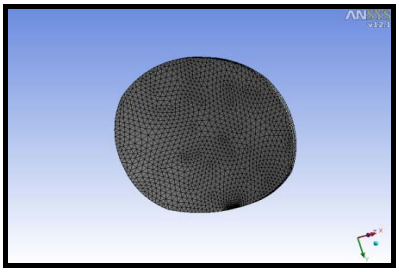

Figure (19) Patella articular cartilages mesh.

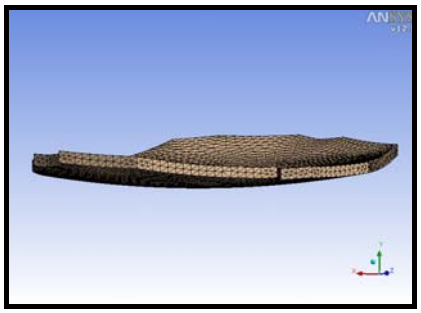

Figure (20) Medial tibia articular cartilage mesh.

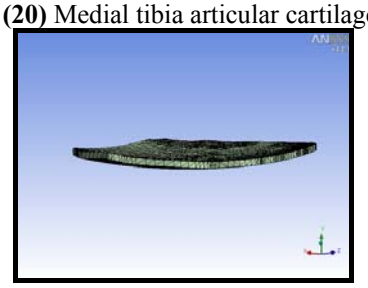

Figure(21) Lateral tibia articular cartilage mesh.

The finite element model meshes for 1, 5, 7.5, and 10 mm are shown in **Figures** (22-27) for different cases.

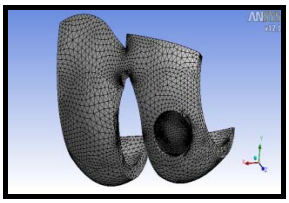

Figure (22) Partial cut without affecting the subchondral bone articular cartilages mesh 10 mm.

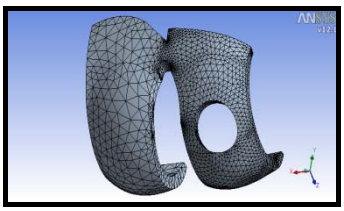

Figure (23) Full cut with part of the subchondral bone articular cartilages models 10 mm.

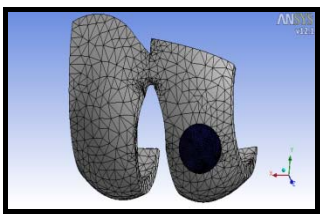

Figure (24) Partial cut without affecting the subchondral bone replaced by using ACI mesh 10 mm.

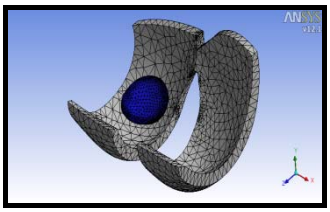

Figure (25) Full cut with part of the subchondral bone replaced by Osteochondral autograft or allograft mesh 10mm

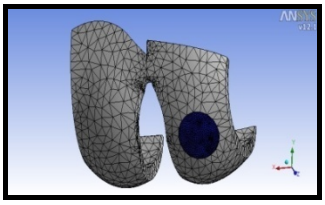

Figure (26) Full cut with part of the subchondral bone replaced by microfracture repair stimulation technique mesh 10 mm.

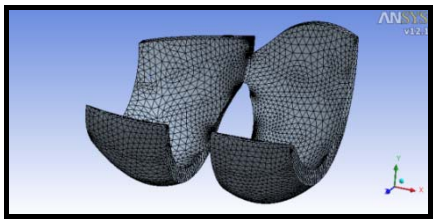

Figure (27) Total replacement of cartilage with (UHMWPE) mesh.

Insert structural loads

Early models to predict the forces across the knee joint are statically indeterminate because the number of independent soft tissue structures acting across the knee joint is greater than what can be solved for using the equations of static equilibrium. However, by making simplifying assumptions in the number of active muscle groups across the joint during a particular activity, it turns out that reasonable estimates of joint reaction forces may be obtained for activities such as walking, stair climbing/descent, squatting, and rising from a chair as shown in Table (3) [S. Kurtz 2004].

Table (3) Summary of average knee joint loading for activities of daily living [S. Kurtz 2004].

Activity	Patello-femoral Joint Force (x BW)	Tibio-femoral Joint Force (x BW)
Walking	0.5	0.4
Squatting	6.0-7.6	2.9-3.5
Rising from a chair	3.1	2.3
Stair climbing /descent	3.3	0.6
Force is expressed in units of body weight (BW).		

The human articular cartilage will be studied in two activities (walking and squatting): In walking the tibiofemoral joint angle is 5^o so the force applied is equal to 0.4 of the body weight. While for patellofemoral joint, the angle is 10^o during walking so the applied force is 0.5 of the body weight. While in squatting , the tibiofemoral joint angle is 122^o so the force applied is equal to 3.5 of the body weight. While for patellofemoral, the joint angle is also 122^o during squatting so the applied force is 7.6 of the body weight [S. Kurtz 2004]. Depending on Table (3), the loads were inserted as a distributed pressure (force over area).

Boundary conditions

The fixed support was applied to the faces of articular cartilage that are connected to bone. In addition, the fluid solid interface was applied to the articular cartilage parts that faced the synovial fluid, this assumption is due to the fact that the fluid flows in and out of the healthy articular cartilages, and a connection between a fluid analysis and structural analysis is done to insert the material properties of the synovial fluid and the porosity and permeability of articular cartilage.

RESULTS

To study the finite element analysis of the articular cartilage, the Von Misses stress, and the total deformation were chosen to be solved. The Stress-Strain Relationship is represented by [B. Nigg 1999]:

$$\{\sigma\} = [D]\ \{\varepsilon\} \qquad (1)$$

where:

$\{\sigma\}$ = stress vector = $[\ \sigma_x\ \sigma_y\ \sigma_z\ \sigma_{xy}\ \sigma_{yz}\ \sigma_{xz}\ ]^T$

[D] = elasticity or elastic stiffness matrix or stress-strain matrix

$\{\varepsilon\}$ = total strain vector = $[\ \varepsilon_x\ \varepsilon_y\ \varepsilon_z\ \varepsilon_{xy}\ \varepsilon_{yz}\ \varepsilon_{xz}\ ]^T$

$$[D]^{-1} = \begin{bmatrix} 1/E_x & -\nu_{xy}/E_x & -\nu_{xz}/E_x & 0 & 0 & 0 \\ -\nu_{yx}/E_y & 1/E_y & -\nu_{yz}/E_y & 0 & 0 & 0 \\ -\nu_{zx}/E_z & -\nu_{zy}/E_z & 1/E_z & 0 & 0 & 0 \\ 0 & 0 & 0 & 1/G_{xy} & 0 & 0 \\ 0 & 0 & 0 & 0 & 1/G_{yz} & 0 \\ 0 & 0 & 0 & 0 & 0 & 1/G_{xz} \end{bmatrix}$$

Also equation (4.1) may be inverted to:

$$\{\varepsilon\} = [D]^{-1}\ \{\sigma\} \qquad (2)$$

The flexibility or compliance matrix, $[D]^{-1}$ is:

(3)

where typical terms are: E_x = Young's modulus in the x direction , ν_{xy} = major Poisson's ratio, ν_{yx} = minor Poisson's ratio, G_{xy} = shear modulus in the xy plane. For orthotropic material transformation for axisymmetric models the input for x-y-z coordinates gives the following stress-strain matrix for the non-shear terms:

$$\left[D_{x-y-z}\right]^{-1} = \begin{bmatrix} 1/E_x & -\nu_{xy}/E_x & -\nu_{xz}/E_x \\ -\nu_{yx}/E_y & 1/E_y & -\nu_{yz}/E_y \\ -\nu_{zx}/E_z & -\nu_{zy}/E_z & 1/E_z \end{bmatrix} \quad (4)$$

The principal stresses (σ_1, σ_2, σ_3) are calculated from the stress componsents by the cubic equation:

$$\begin{vmatrix} \sigma_x - \sigma_0 & \sigma_{xy} & \sigma_{xz} \\ \sigma_{xy} & \sigma_y - \sigma_0 & \sigma_{yz} \\ \sigma_{xz} & \sigma_{yz} & \sigma_z - \sigma_0 \end{vmatrix} = 0 \quad (5)$$

where: σ_o = principal stress (3 values)
The three principal stresses are labeled σ_1, σ_2, and σ_3. The principal stresses are normal stresses, acting on principal planes on which the shearing stresses are zero, and are calculated by using the existing six normal and shearing stress components σ_x, σ_y, σ_z, τ_{xy}, τ_{xz}, and τ_{yz}.

The principal stresses are ordered so that σ_1 is the most positive (tensile) and σ_3 is the most negative (compressive).The stress intensity σ_I is the largest of the absolute values of σ_1- σ_2, σ_2- σ_3, or σ_3 - σ_1.
That is:

$$\sigma = \text{MAX}\left(|\sigma_1 - \sigma_2| |\sigma_2 - \sigma_3| |\sigma_3 - \sigma_1|\right) \quad (6)$$

The von Mises or equivalent stress σ_e is computed as:

$$\sigma_e = \left(\frac{1}{2}\left[(\sigma_1 - \sigma_2)^2 + (\sigma_2 - \sigma_3)^2 + (\sigma_3 - \sigma_1)^2\right]\right)^{\frac{1}{2}} \quad (7)$$

Or

$$\sigma_e = \left(\frac{1}{2}\left[(\sigma_x - \sigma_y)^2 + (\sigma_y - \sigma_z)^2 + (\sigma_z - \sigma_x)^2 + 6(\sigma^2_{xy} + \sigma^2_{yz} + \sigma^2_{xz})\right]\right)^{\frac{1}{2}} \quad (8)$$

Normal Models Results

For normal articular cartilage, the results were taken for each model in two activities (walking and squatting) represented as a contour in the **Figures** (29-39).

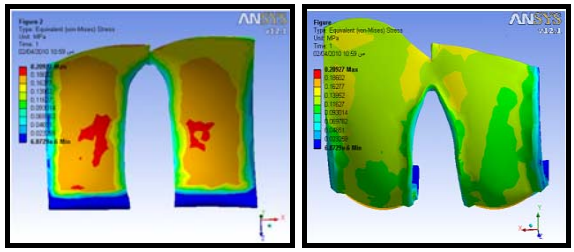

(a) Top view (b) Front view

Figure (29) Von Mises stress for normal distal femur articular cartilage during walking.

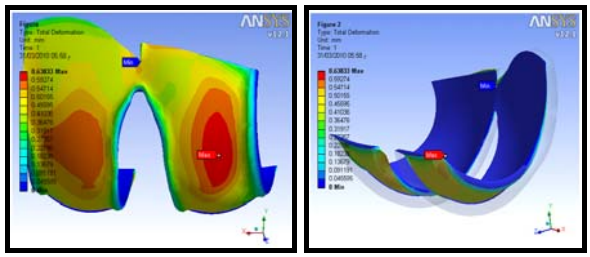

(a) Front view (b) Isometric view

Figure (30) Total deformation for normal distal femur articular cartilage during walking.

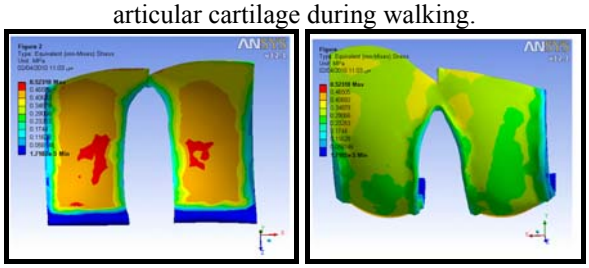

(a) Top view (b) Front view

Figure (31) Von Mises stress for normal distal femur articular cartilage during squatting.

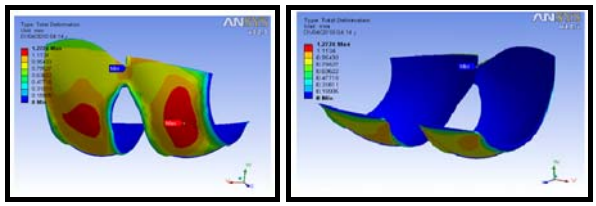

(a) Front view (b) Isometric view

Figure (32) Total deformation for normal distal femur articular cartilage during squatting.

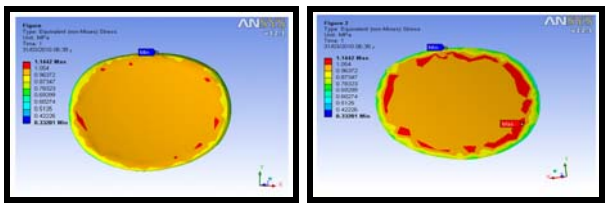

(a) front view (b) back view

Figure (33) Von Mises stress for normal patella articular cartilage during walking.

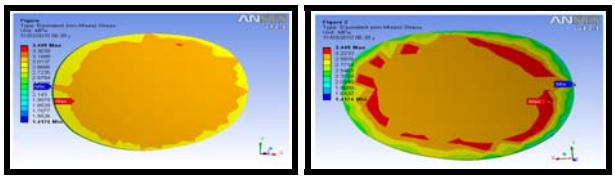

(a) Front view (b) Back view

Figure (34) Von Mises stress for normal patella articular cartilage during squatting.

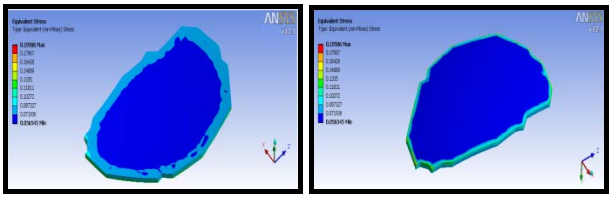

(a) Top view (b) Bottom view

Figure (35) Von Mises stress for normal medial tibia articular cartilage during walking.

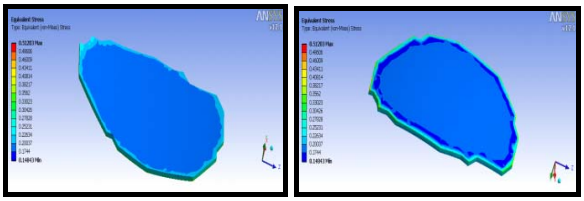

(a) Top view (b) Bottom view

Figure (36) Von Mises stress for normal medial tibia articular cartilage during squatting.

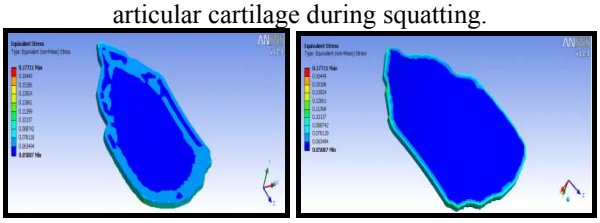

(a) Top view (b) Bottom view

Figure (37) Von Mises stress for normal lateral tibia articular cartilage during walking.

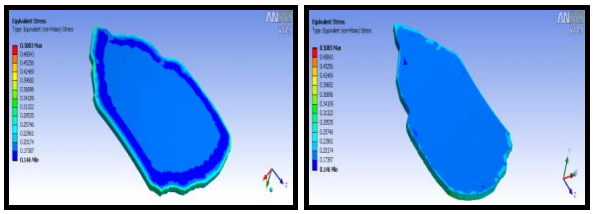

(a) Top view (b) Bottom view

Figure (38) Von Mises stress for normal lateral tibia articular cartilage during squatting.

Table (4) Maximum Von Mises stress for normal articular cartilage models during walking and squatting.

No.	Model	Maximum Von Mises stress (MPa)	
		Walking	Squatting
1	Distal femur	0.20927	0.52318
2	Patella	1.1442	3.449
3	Medial tibia	0.19506	0.51203
4	Lateral tibia	0.17711	0.5083

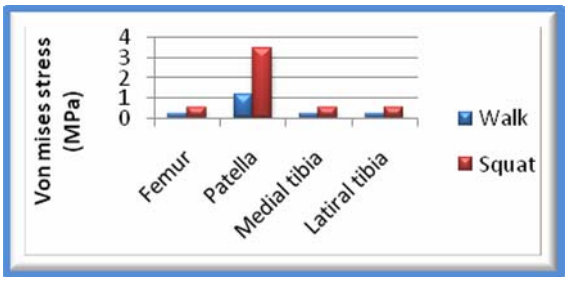

Figure (39) Maximum Von Mises stress for normal articular cartilage models during walking and squatting.

Osteoarthritic articular cartilage

For Partial cut without affecting the subchondral bone it can be see that there is a big difference between normal and osteoarthritic articular cartilage stresses even when the defect is just 1 mm, and this is be so obvious in the squatting. In the four models, the maximum stress is on the sides of the cut parts and increases with increasing the cut diameter. For total deformation result, it can be seen that there is no or small deformation in the cut parts but it is the maximum in the peripheral parts as shown in **Figures** (40-43).

While for Full cut with part of the subchondral bone it's obvious the big differences are between the normal and full cut defective articular cartilages stresses, especially in squatting. In the three models, the maximum stress is on the sides of the cut parts and its increases with increasing the cut diameter. For total deformation results, the maximum deformation is in the peripheral parts of the cuts and there is no deformation in the cartilage - bone interface. The percentage for two types of Osteoarthritic articular cartilage close to normal are 19% for walking and 16% for squatting, as shown in **Figures** (44-46).

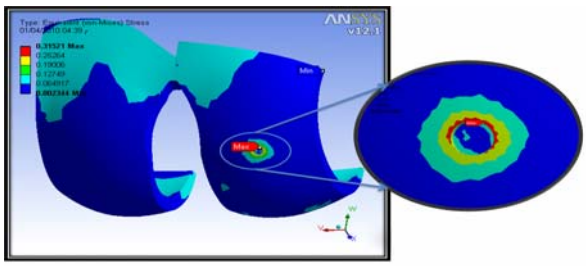

Figure (40) Von Mises stress for 1mm partial cut articular cartilage during walking.

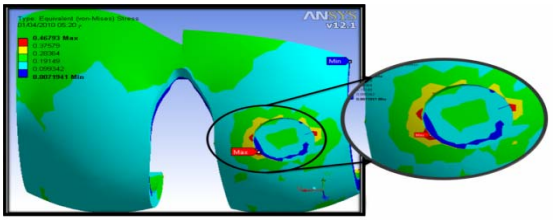

Figure (41) Von Mises stress for 7.5 mm partial cut articular cartilage during walking.

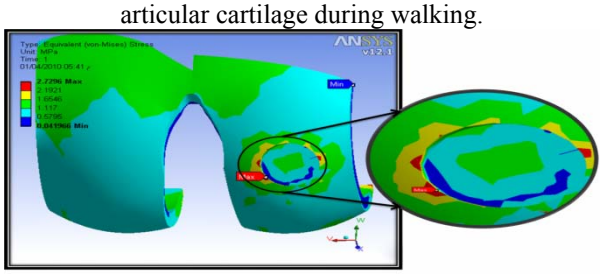

Figure (42) Von Mises stress for 7.5 mm partial cut articular cartilage during squatting.

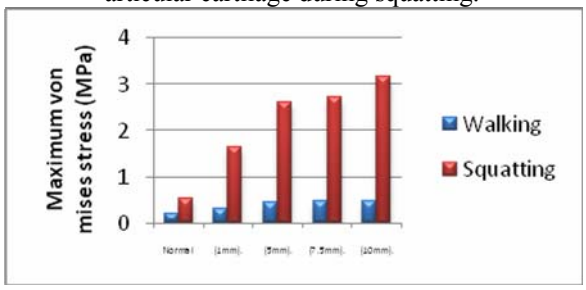

Figure (43) Maximum Von Mises stress for osteoarthritic articular cartilage with Partial cut without affecting the subchondral bone models during walking and squatting.

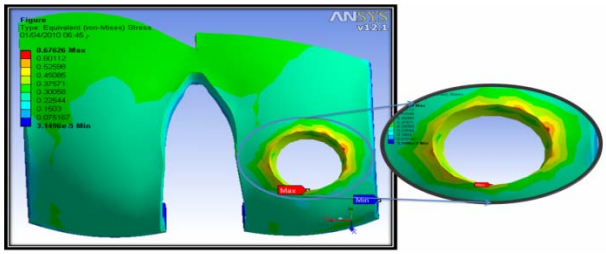

Figure (44) Von Mises stress for 7.5 mm full cut articular cartilage during walking.

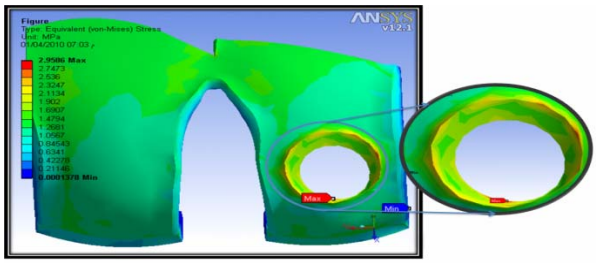

Figure (45) Von Mises stress for 7.5 mm full cut articular cartilage during squatting.

Table (5) Maximum Von Mises stress for osteoarthritic articular cartilage models during walking and squatting.

No.	Model	Maximum Von Mises stress (MPa)	
		Walking	Squatting
1	Partial cut without affecting the subchondral bone (1mm).	0.31521	1.6549
2	Partial cut without affecting the subchondral bone (5mm).	0.44807	2.6138
3	Partial cut without affecting the subchondral bone (7.5mm).	0.46793	2.7296
4	Partial cut without affecting the subchondral bone (10mm).	0.48082	3.1554
5	Full cut with part of the subchondral bone (5 mm).	0.6554	2.8483
6	Full cut with part of the subchondral bone(7.5 mm).	0.67626	2.9586
7	Full cut with part of the sub chondral bone(10 mm).	0.71384	3.2387

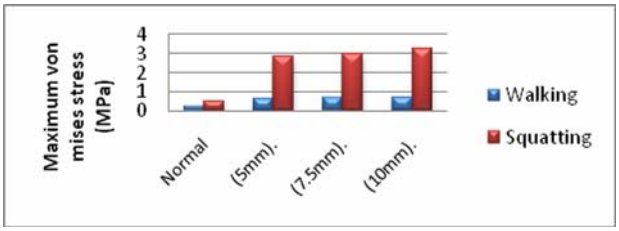

Figure (46) Maximum Von Mises stress for osteoarthritic articular cartilage with full cut with part of the subchondral bone models during walking and squatting.

Artificial articular cartilages models

For Partial cut without affecting the subchondral bone replaced by using autologous chondrocyte implantation (ACI), It can be seen that the maximum stresses for the artificial articular cartilage is very close to the normal articular cartilage but it is concentrated in the artificial part. The advantages and disadvantages of this technique are shown in **Figures** (47-49). The percentage for how ACI close to normal is 87.50% for walking and 90% for squating.

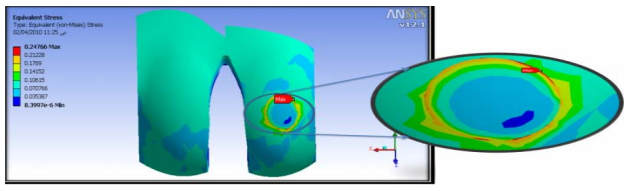

Figure (47) Von Mises stress for 7.5 mm artificial articular cartilage replaced by using (ACI) during walking.

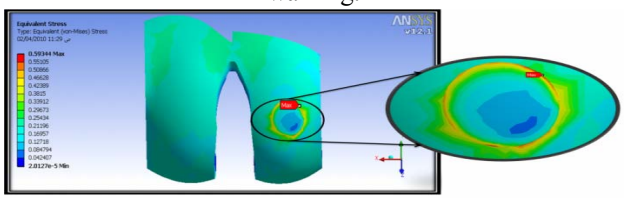

Figure (48) Von Mises stress for 7.5 mm artificial articular cartilage replaced by using (ACI) during squating.

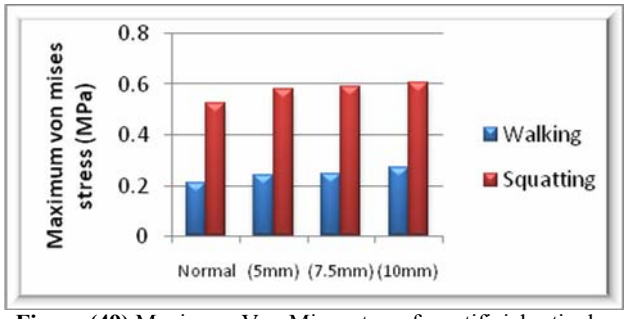

Figure (49) Maximum Von Mises stress for artificial articular cartilage replaced by using autologous chondrocyte implantation (ACI) during walking and squatting.

For Full cut with part of the subchondral bone replaced by Osteochondral autograft or allograft. The maximum stresses concentrated in the artificial part. The advantages and disadvantages of this technique are shown in **Figure**(50-52). The percentage for how osteochondral autograft or allograft close to normal is 61% for walking and 17% for squating.

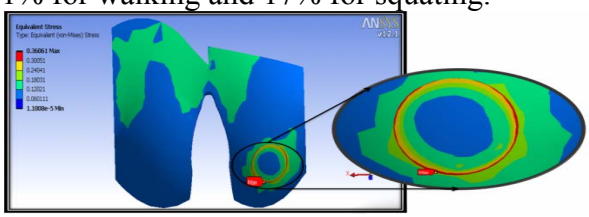

Figure (50) Von Mises stress for 7.5 mm artificial articular cartilage replaced by graft during walking.

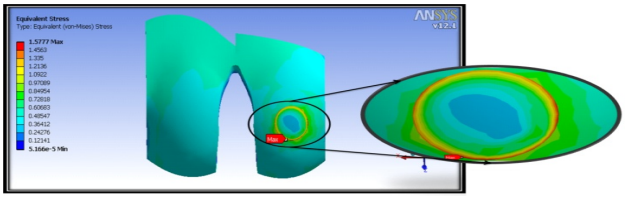

Figure (51) Von Mises stress for 7.5 mm artificial articular cartilage replaced by graft during squating.

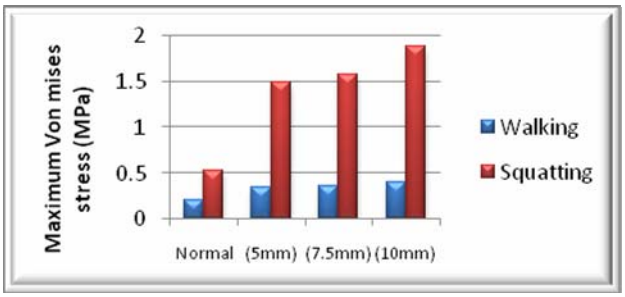

Figure (52) Maximum Von Mises stress for artificial articular cartilage replaced by osteochondral autograft or allograft during walking and squatting.

For Full cut with part of the subchondral bone replaced by using Microfracture Repair stimulation technique, The maximum stress for the artificial articular cartilage is greater than that of the normal articular cartilage especially in squatting but it is still lower than when it defected. The maximum stresses are concentrated in the artificial part. The advantages and disadvantages of this technique are shown in **Figures** (53-55). The percentage for how Microfracture technique close to normal is 51% for walking and 26.5% for squating.

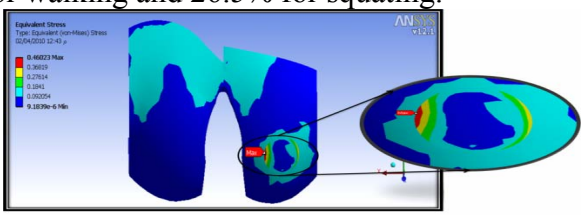

Figure (53) Von Mises stress for 7.5mm artificial articular cartilage replaced by using microfracture repair stimulation technique during walking.

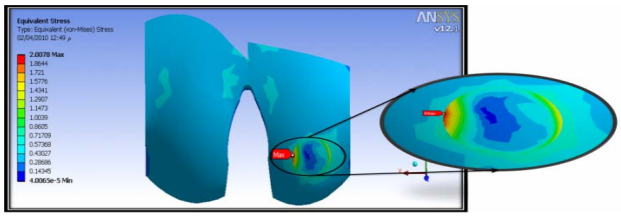

Figure (54) Von Mises stress for 7.5 mm artificial articular cartilage replaced by using microfracture repair stimulation technique during squatting.

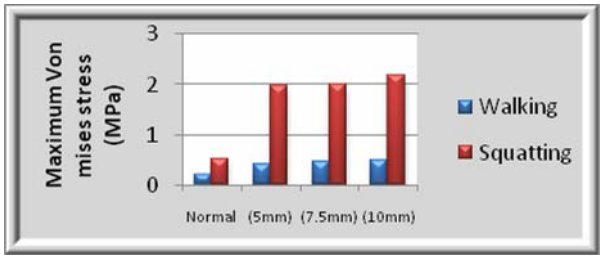

Figure (55) Maximum Von Mises stress for artificial articular cartilage replaced by using microfracture repair stimulation technique during walking and squatting.

Total replacement of cartilage with ultra high molecular weight polyethylene (UHMWPE), It can be seen that the maximum stress for the artificial articular cartilage is not very close to the normal articular cartilage but it is much better than the osteoarthritic articular cartilage. The maximum stress is on the sides of artificial articular cartilage and this is due to the thickness differences between the sides and the middle as shown in **Figures** (56-58).

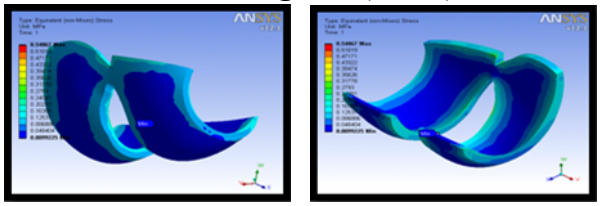

(a) front view (b) back view

Figure (56) Von Mises stress for total replacement of cartilage with ultra high molecular weight polyethylene (UHMWPE) during walking.

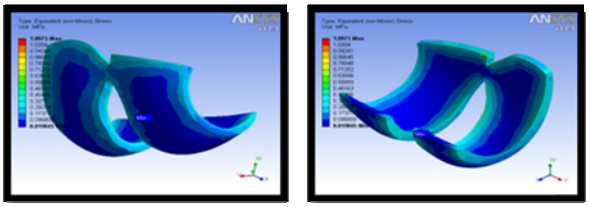

(a) front view (b) back view

Figure (57) Von Mises stress for total replacement of cartilage with ultra high molecular weight polyethylene (UHMWPE) during squatting.

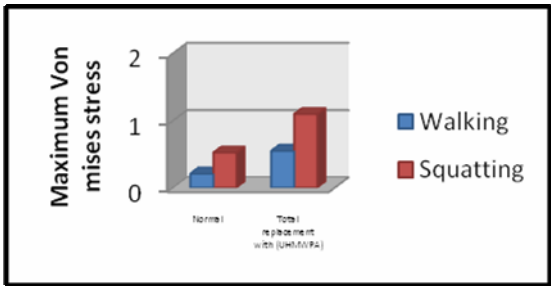

Figure (58) Maximum Von Mises stress for total replacement of cartilage with ultra high molecular weight polyethylene (UHMWPE) during walking and squatting.

Table (6) Maximum Von Mises stress for artificial articular cartilage models during walking and squatting.

No.	Model	Maximum Von Mises stress (MPa)	
		Walking	Squatting
1	Partial cut without affecting the subchondral bone replaced by using ACI (5 mm)	0.23909	0.58064
2	Partial cut without affecting the subchondral bone replaced by using ACI (7.5 mm)	0.24766	0.59344
3	Partial cut without affecting the subchondral bone replaced by using ACI (10 mm)	0.27011	0.60775
4	Full cut with part of the subchondral bone replaced with Osteochondral autograft or allograft (5mm)	0.34272	1.4994
5	Full cut with part of the subchondral bone replaced with Osteochondral autograft or allograft (7.5mm)	0.36061	1.5777
6	Full cut with part of the subchondral bone replaced with Osteochondral autograft or allograft (10mm)	0.39666	1.8932
7	Full cut with part of the subchondral bone replaced by using Microfracture Repair stimulation technique (5mm)	0.41223	1.9744
8	Full cut with part of the subchondral bone replaced by using Microfracture Repair stimulation technique (7.5mm)	0.46023	2.0078
9	Full cut with part of the subchondral bone replaced by using Microfracture Repair stimulation technique (10mm)	0.49869	2.1866
10	Total replacement of cartilage with ultra high molecular weight polyethylene (UHMWPE)	0.54867	1.0973

Conclusions

1. The maximum stress of normal articular cartilage is in cartilage-bone interface during walking and squatting, but the stress is reach the double during squatting, which means the stress is increasing with knee flexion angle increasing. Also, the maximum stress in the patellar articular cartilage is greater than that in the other knee joint articular cartilages specially in squatting because the load reaches 7.6 of

the total body weight on the patella articular cartilage.

2. For the autologous chondrocyte implantation, the maximum stress for the artificial articular cartilage is very close to the normal articular cartilage. It represents the best results for replacement but it needs two operations and cannot be useful for older patients or for patients with deep osteoarthritis.

3. For osteochondral autograft, allograft, or microfracture repair stimulation technique for replacement, the maximum stress of the artificial articular cartilage is greater than that of the normal articular cartilage but it is still lower than when it is defected.

4. For total replacement of cartilage with UHMWPE, the maximum stress for the artificial articular cartilage is not very close to the normal articular cartilage but it is much better than the osteoarthritic articular cartilage. The maximum stress is on the sides of artificial articular cartilage, this is due to the thickness differences between the sides and the middle.

REFERENCES

Abhijit M. Bhosale, and James B. Richardson, "Articular Cartilage: Structure, Injuries And Review Of Management", Institute of Orthopaedics and Arthritis Research Centre, UK, British Medical Bulletin; 87: 77–95, 2008.

Arif Iftekhar, "Standard Handbook Of Biomedical Engineering And Design", University of Minnesota, Minneapolis, The McGraw-Hill Companies, chapter 12, 2004.

Ateshian G A, and Hung C T, "The Natural Synovial Joint: Properties Of Cartilage", Proc. IMechE Vol. 120 Part J: J. Engineering Tribology, 2006.

Benno M. Nigg, and Walter Herzog, "Biomechanics of the Musculo-Skeletal System", University of Calgary, Calgary, Alberta, Canada, second edition, p. 86-105, 1999.

Constantin Bratianu, Paul Rinderu, and Lucian Gruionu," A 3D Finite Element Model of a Knee for Joint Contact Stress Analysis during Sport Activities", Key Engineering Materials Trans Tech Publications, Switzerland, Vols. 261-263, pp 513-518, 2004.

Daniel J. Schneck, Joseph D. Bronzino, "Biomechanics Principles And Applications", Boca Raton London New York Washington, D.C., 2003.

Dennis R. Carter, Gary S. Beaupré, Marcy Wong, R. Lane Smith, Tom P. Andriacchi, and David J. Schurman, "The Mechanobiology of Articular Cartilage Development and Degeneration", pp. S69–S77, Lippincott Williams & Wilkins, 2004.

Felson DT, Zhang Y, Hannan MT, Naimark A. Weissman B, and Aliabadi P., "Risk factors for incident radiographic knee osteoarthritis in the elderly", Arthr Rheum, 22:716-733, 1997.

Gelse K., Olk A., Eichhorn S., Swoboda B., Schoene M., and Raum K., "Quantitative Ultrasound Biomicroscopy For The Analysis Of Healthy And Repair Cartilage Tissues", Germany, Vol. 11, p. (58-71) , 2010.

Guoan Li, Orlando Lopez, "Reliability Of A 3D Finite Element Model Constructed Using Magnetic Resonance Images Of A Knee For Joint Contact Stress Analysis", Harvard Medical School, Boston, 1998.

Janssen P.J.F.M., "Influence of Excessive Loading on The Mechanical Properties of Articular Cartilage", Technical University Eindhoven, 2004.

Jiang Yao, Art D. Salo, Monica Barbu-McInnis, and Amy L. Lerner, "Finite Element Modeling Of Knee Joint Contact Pressures And Comparison To Magnetic Resonance Imaging Of The Loaded Knee", Washington, D.C., November 16-21, 2003.

Jonathan Black, and Garth Hastings, "Handbook of Biomaterial Properties", First edition, Chapman & Hall, London, 1998.

Matej Mlejnek, "Medical Visualization for Orthopedic Applications", Ph.D., Institute of Computer Graphics and Algorithms, Vienna University of Technology, Austria, 2006.

Michele J. Grimm, "Standard Handbook Of Biomedical Engineering And Design", Detroit, Michigan, The McGraw-Hill, chapter 15,2004.

Orthopod, "A Patient's Guide to Articular Cartilage Problems of the Knee", 116 West Main St., Suite D, Missoula, MT 59802-2295, , Medical Multimedia Group, LLC, 2003.

Ramaswamy Krishnan, Seonghun Park, Felix Eckstein, Gerard A. Ateshian, "Inhomogeneous Cartilage Properties Enhance Superficial Interstitial Fluid Support and Frictional Properties", Journal of Biomechanical Engineering, Vol. 115, 2003.

Richard Baxter, "Articular Cartilage Injuries and Management", 2008.

Sam Leffler, Glenn Randers, Andreas Dilger, Guy Eric Schalnat, Jean-loup Gailly, Mark Adler, David E. Steward, and Zbigniew Leyk, "ANSYS 12.1 Inc. Theory Reference", ANSYS Inc., Southpointe, 2009.

Seeley−Stephens−Tate, "Anatomy and Physiology", Sixth Edition, McGraw−Hill Companies, p. 114-126, 146, 2004.

Stephen D. Fening, "The Effects Of Meniscal Sizing On The Knee Using Finite Element Methods", Ph. D. thesis, Ohio University, 2005.

Steven M. Kurtz, "The UHMWPE Handbook", Principal Engineer, Elsevier Academic Press, 2004.

Sven Knecht, "Biomechanical Assessment of Native and Tissue Engineered Articular Cartilage", Ph.D., Dipl. Ing., University Stuttgart, Citizen of Germany, 2006.

Tamara K. Pylawka, Richard W. Kang, Brian J. Cole, "Articular Cartilage Injuries", chapter 30, 2004.

Thomas J. Gill, Peter D. Asnis, Eric M. Berkson, "The Treatment of Articular Cartilage Defects Using the Microfracture Technique", Journal of Orthopaedic, 18(10):716-738, 2006.

Thor F. Besier, Garry E. Gold, Gary S. Beaupré, And Scott L. Delp, "A Modeling Framework to Estimate Patellofemoral Joint Cartilage Stress In Vivo", Medicine and Science In Sports and Exercise, American College of Sports Medicine, 2005.

Ulrich Meyer, and Hans Peter Wiesmann, "Bone and Cartialge Engineering", Springer, 2006.

Van De Graaff, "Human Anatomy", Sixth Edition, McGraw−Hill Companies, p.117-130, 2001.

Wendell S. Holmes Jr, "Articular Cartilage Injuries in the Athlete's Knee: Current Concepts in Diagnosis and Treatment", Columbia, 2004.

William Bogatay, "Finite Element Analysis of Knee Cartilage with an Osteochondral Graft", Mechanical Engineering, The Ohio State University, 2009.

Wouter Wilson, "An Explanation for the Onset of Mechanically Induced Cartilage Damage", Ph.D., Technische Universiteit Eindhoven, 2005.